Desalination 345 (2014) 94–100

Contents lists available at ScienceDirect

Desalination

journal homepage: www.elsevier.com/locate/desal

Cation exchange copolymer enhanced electrosorption

Benjamin M. Asquith [a], Jochen Meier-Haack [b], Bradley P. Ladewig [a,*]

[a] Department of Chemical Engineering, Monash University, VIC 3800, Australia
[b] Leibniz Institute of Polymer Research Dresden, Hohe Strasse 6, 01069 Dresden, Germany

HIGHLIGHTS

- Activated carbon electrodes were coated with sulfonated random copolymers.
- Coating layer resistance did not adversely affect the build up of charge.
- Electrode capacitance was enhanced by polymers with a high ion-exchange capacity.
- Coating thickness influences the resistance of the carbon electrodes.

ARTICLE INFO

Article history:
Received 18 February 2014
Received in revised form 18 April 2014
Accepted 19 April 2014
Available online 13 May 2014

Keywords:
Capacitive deionisation
Cation-exchange polymer
Activated carbon
Cyclic voltammetry
Electrochemical impedance spectroscopy

ABSTRACT

In this study the effects of cation exchange polymer coatings on activated carbon electrodes for capacitive deionization (CDI) were investigated. Electrodes were fabricated from activated carbon, graphite and PVDF, then coated with sulfonated poly(arylene ether sulfone) random copolymers. Additional resistance was created by the coating layer, however compared with the uncoated electrodes the coatings did not significantly affect the rate of charge build up. Electrochemical impedance spectroscopy (EIS) results indicated that both capacitance and charging resistance are influenced by polymer conductivity, water uptake and the thickness of the coating layer. The results also indicated that in addition to functioning as a superficial charge barrier, copolymer that penetrates into the carbon substrate might offset the loss in capacitance caused by PVDF binder pore blockage.

1. Introduction

Capacitive deionization (CDI) is a developing desalination technology that can be used for the highly efficient desalination of brackish water, the production of ultra pure water, water softening and the removal of other charged impurities from water streams [1–3]. It is an electrosorption process that relies on the formation of an electrical double layer on a porous, polarizable electrode. This buildup of charge creates a similar buildup of oppositely charged ions from an electrolyte solution at the electrode–solution interface, thereby removing salt ions from solution.

Activated carbon is an attractive material for electrosorption due to its relatively low cost and large specific surface area, typically in the order of 1000–2000 m^2/g, and numerous studies have focused on its use for CDI [4–12]. Unfortunately the potential for activated carbon to adsorb salt ions from solution is hindered by its microporous nature, low conductivity, and high electrical and mass transfer resistances [13]. Furthermore, it typically exhibits a randomly arranged pore network that may hinder ion movement and thus sorption [14]. As such, research efforts to improve its electrosorption capacity and efficiency are ongoing, with techniques such as surface modification and the incorporation of membranes. The modification of the activated carbon surface has been shown to improve electrosorption efficiency by neutralising polar surface charges thereby reducing unwanted physical adsorption. Studies have shown that enhanced performance can be achieved through chemical surface modification of activated carbons with titanium [15,16], titanium dioxide nanoparticles [5], potassium hydroxide and nitric acid [17,18], and zinc oxide nanorods [19].

In addition to the drawbacks of activated carbon, an inherent disadvantage of the CDI process is that during the adsorption of counter-ions, a simultaneous desorption of co-ions occurs. Thus, for each electron passing through the external circuit, less than one salt molecule is adsorbed [20–23]. To restrict this co-ion movement during adsorption, ion exchange membranes may be placed in front of each electrode. This is known as membrane capacitive deionization (MCDI), and was first introduced by Andelman and Walker in 2004 [24]. It has been shown to significantly increase salt adsorption and energy efficiency by improving the efficiency of counter-ion adsorption [25–30]. Ion exchange membranes also allow for the application of a reverse potential

* Corresponding author.
E-mail address: bradley.ladewig@monash.edu (B.P. Ladewig).

http://dx.doi.org/10.1016/j.desal.2014.04.027
0011-9164/

during the desorption phase, allowing for a greater depletion of ions at the electrode and thus greater adsorption capacity in the following cycles [31].

Commercial cation exchange membranes used for MCDI include Neosepta CM-1 [25] and Neosepta CMX [32–34]. These membranes are poly(vinyl chloride) based with styrene/divinylbenzene copolymers and are designed for desalination purposes with high permselectivity, low electrical resistance, and high mechanical stability [35]. However, the use of flat sheet membranes creates additional resistance between the membrane and the electrode. One alternative approach to reduce this resistance involved the spraying of carbon cloth electrodes with bromomethylated poly(2, 6-dimethyl-1,4-phenylene oxide) (BPPO) solution, which was subsequently sulfonated with sulfuric acid to attach functional groups to the polymer [34]. Another approach by Kim et al. [36] saw the coating of carbon electrodes with poly(vinyl alcohol), which was sulfonated and crosslinked by using sulfosuccinic acid. This technique yielded ion-exchange coatings with area specific resistances lower than those of commercial membranes.

The poly(arylene ether sulfone) copolymers used in this study are characterised by having high conductivity and mechanical stability. Similar ion-exchange copolymers have been developed for pressure-driven desalination membranes and for fuel cell applications [37–44], but few studies have focused on their application for CDI [45]. In this work these cation exchange polymers have been applied as thin membrane coatings to activated carbon electrodes in order to enhance electrosorption performance. The characteristics of the coated electrodes are compared to uncoated electrodes, and correlations between the polymer properties and electrode performance are highlighted. In particular, the influence of conductivity and water uptake on resistance and capacitance is discussed.

2. Experimental

2.1. Materials

4,4′-difluorodiphenyl sulfone was purchased from FuMA-Tech GmbH (Germany) and was purified by vacuum distillation. 4,4′-dihydroxydiphenyl sulfone (DHDPhS), N-methyl-2-pyrrolidone (NMP), poly(vinylidene) fluoride) (PVDF), activated carbon and graphite powder were purchased from Sigma-Aldrich (Australia). Concentrated sulfuric acid (min. 96%) was obtained from Acros (Belgium). 2,5-diphenylhydroquinone (DPhHQ) was prepared as per the procedure described by Vogel et al. [43].

2.2. Polymer synthesis and sulfonation

Three random copolymers were synthesised by using the silyl-method as per the procedure previously described [43,45]. The ratio of the monomers in the random copolymers was varied such that the monomer ratio of DPhHQ to DHDPhS was 6:4 for RCP 1, 5:5 for RCP 2 and 4:6 for RCP 3. All polymers were sulfonated by using concentrated sulfuric acid (96–98%). The molecular structure of the random copolymers can be seen in Fig. 1.

2.3. Electrode preparation

Using NMP as a solvent, a slurry consisting of activated charcoal, graphite powder as conductive material and PVDF as a binder was prepared such that the final (dry) content of the electrode was 75 wt.% activated charcoal, 15 wt.% graphite and 10 wt.% PVDF. The slurry was coated onto graphite sheets to a thickness of 200 μm using a doctor blade and dried in a vacuum oven for 24 h at 120° to completely remove the solvent.

Polymer coated electrodes were prepared by first dissolving the sulfonated polymers in NMP such that the concentration was 15 wt.%. The solutions were cast onto the carbon electrodes and dried under vacuum for 2 h at 60 °C, then for a further 24 h at 80 °C. The samples were rinsed with distilled water to remove residual NMP, soaked in 0.5 M NaCl to convert the polymer to the Na^+ form, then rinsed again with water to remove excess NaCl from the polymer matrix.

2.4. Electrode characterisation

Specific surface area and pore size distribution were measured on a Micrometrics ASAP 2020 Physisorption Analyser using N_2 as the adsorbate at 77 K. FTIR spectra were collected by using a PerkinElmer Spectra 100 to confirm the chemical structure of the cation exchange polymer coatings. Cyclic voltammetry experiments were performed by using a Biologic VSP potentiostat connected to a three-electrode electrochemical cell. The working electrode was the carbon material to be tested with an exposed surface area of 0.785 cm^2. The reference electrode was a saturated Ag/AgCl KCl electrode, and the counter electrode was a platinum mesh electrode. Electrochemical Impedance Spectroscopy (EIS) was performed by using the same three-electrode cell over the frequency range 10 mHz to 1 MHz, with an applied voltage amplitude of 10 mV.

3. Results & discussion

3.1. Activated carbon surface area & pore size distribution

The isotherm obtained for the activated carbon is shown in Fig. 2. The large increase in adsorbed gas at low relative pressure is a typical Type I isotherm for a microporous solid [46]. The pore size distribution for the activated carbon, also shown in Fig. 2, confirms the microporous nature of the carbon, with a single peak at 0.7–0.8 nm. The gradual uptake from a relative pressure of around 0.2 indicates some mesopores, although as seen in the pore size distribution, these do not contribute greatly to the specific surface area of the carbon.

Due to the microporous nature of the carbon, the BET specific surface area was calculated by using data from the relative pressure range 0–0.08, such that the value $Q(P_0–P)$ increased with relative pressure P/P_0 (where Q is the volume of gas adsorbed, P is the measured pressure and P_0 is the

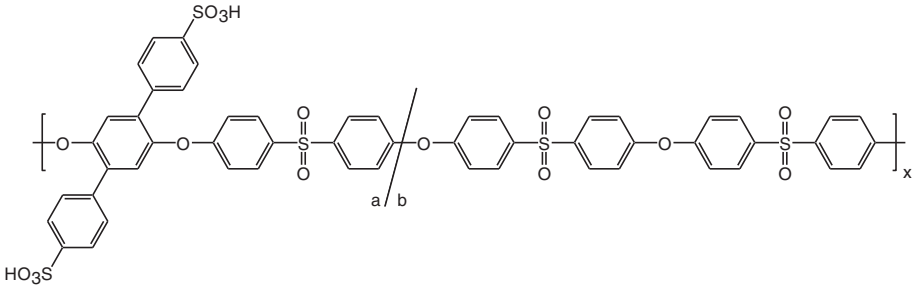

Fig. 1. Repeating unit of the random copolymer. RCP 1: a = 6, b = 4; RCP 2: a = 5, b = 5; RCP 3: a = 4, b = 6.

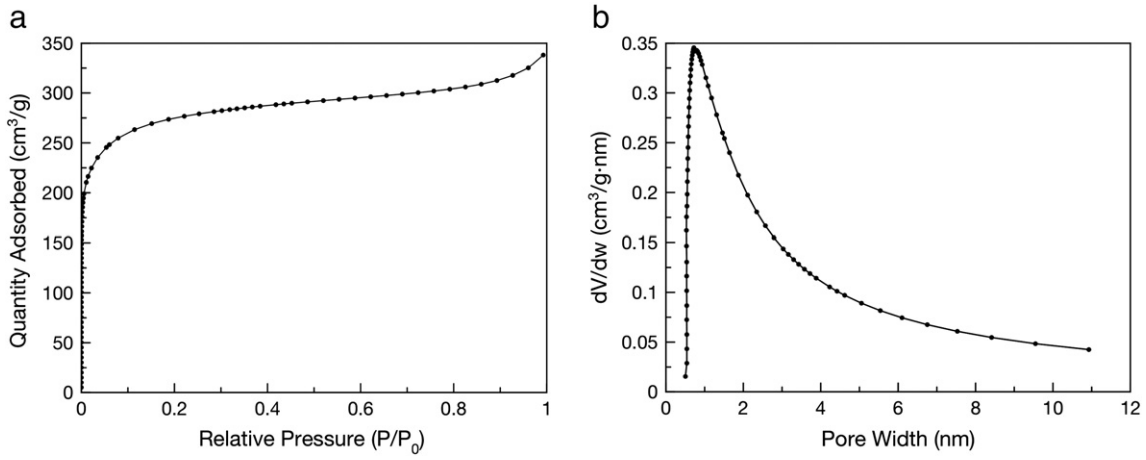

Fig. 2. a) Activated carbon adsorption isotherm and b) pore size distribution, measured by physical adsorption.

saturation pressure) [47]. The specific surface area was calculated to be 1043 m^2/g. The conductive graphite filler was calculated to have a specific surface area of 21.1 m^2/g, and thus is considered to have negligible impact on the adsorption of ions.

3.2. Electrode morphology

The properties of the random copolymers are presented in Table 1. All electrodes were tested for hydro- and thermal stability by placing them in water at 80 °C for 6 h. No degradation was observed, no carbon was removed from the surface of the uncoated electrodes, and all polymers adhered strongly to the carbon such that they were not removed after water treatment. Furthermore, all electrodes were stored in water at room temperature before use, with no loss of carbon or polymer observed. Due to the adhesion of the coating layer to the carbon electrode, the polymer acts as a pseudo-binder, providing additional mechanical strength.

Fig. 3 shows SEM images of both uncoated and coated carbon electrodes. Discrete carbon and graphite powder particles are observed in Fig. 3a, while in Fig. 3b the polymeric coating is seen to cover the entire electrode, analogous to placing a dense phase ion exchange membrane directly against the carbon electrode.

FTIR analysis was used to confirm successful coating of carbon electrodes by comparison with uncoated carbon electrodes and flat sheet membranes cast from the same copolymers. Fig. 4 shows the FTIR spectra of uncoated electrodes (a), coated electrodes (c–e) and a flat sheet membrane cast from RCP 1 (b). As the same precursor monomers are used for each of the random copolymers, their molecular structures differ only in the ratio of the statistically distributed monomers. Hence, each random copolymer membrane spectrum exhibited the same peaks.

C═C stretching vibrations from aromatic rings are represented by peaks at 1580 cm^{-1} and 1485 cm^{-1}. Peaks at 1300 cm^{-1} and 1146 cm^{-1} are S═O stretching vibrations from the sulfone group, while the small peak at approximately 1170 cm^{-1} indicates an S═O stretching vibration on the sulfonated side-chains. Peaks below 1000 cm^{-1} are attributed to the S–O stretch of the sulfonate group and C–H bending on the aromatic ring. The matching spectra of the coated electrodes for all three random copolymers, in addition to the distinct difference between the coated and uncoated electrodes, confirms the successful application of the polymer onto the carbon substrate.

Table 1
Polymer coating properties. Data from [45].

Polymer coating	IEC (mmol/g)	Water uptake (%)*	Conductivity (mS/cm)**	Contact angle (degrees)	Transport number
RCP 1	2.05	49.9	15.13	30.3	.94
RCP 2	1.73	35.7	8.36	38.2	.99
RCP 3	1.44	26.4	3.79	46.1	.98

* Measured in the Na + form.
** In-plane conductivity.

3.3. Electrochemical analysis — Cyclic voltammetry

Cyclic voltammetry was used to measure specific capacitance. From the measured current, the specific capacitance of the activated carbon, C (F/g activated carbon), was calculated by using the following equation [48]:

$$C = \frac{i}{mv}$$

Where i is the current (A), m is the mass of carbon (g) and v is the scan rate (V/s). The capacitance of uncoated electrodes as a function of potential measured at scan rates of 5 mV/s and 20 mV/s can be seen in Fig. 5. At both the fast and slow scan rates, a rectangular shape is observed, indicating the formation of an electrical double layer at the carbon-solution interface and the successful adsorption/desorption of ions. Due to the high microporosity of the carbon, a greater capacitance is observed at 5 mV/s, as the slower scan rate allows greater time for ion transport into the micropores.

A comparison of the capacitance of uncoated electrodes and electrodes coated with the random copolymers at scan rates of 5 mV/s and 20 mV/s can be seen in Fig. 6. At 20 mV/s (Fig. 6a, c and e) during the forward scan there is no enhancement in capacitance compared to the uncoated samples. However, during the reverse scan at potentials lower than approximately 200 mV an appreciable difference in capacitance between the uncoated and coated samples is observed. Similarly, for both the forward and reverse scans at 5 mV/s (Fig. 6b, d and f), the build-up of charge on the coated samples is seen to be better than the uncoated samples. This improved performance is attributed to a greater expulsion of cations during the forward scan and restricted anion movement during the reverse scan as the electrode becomes negatively charged.

For electrodes coated with RCP 2 and RCP 3 (Fig. 6c–f), slower increases in capacitance compared to the uncoated samples are observed at both scan rates when the scan direction changes. Due to the increased resistance provided by the coating layer, this effect is more pronounced at 20 mV/s when there is less time for the ions to diffuse through the polymer matrix. At 5 mV/s the ions have more time to diffuse through the polymer and into the pores of the activated carbon, thus reducing the effect of the additional coating resistance. Additionally, at 5 mV/s

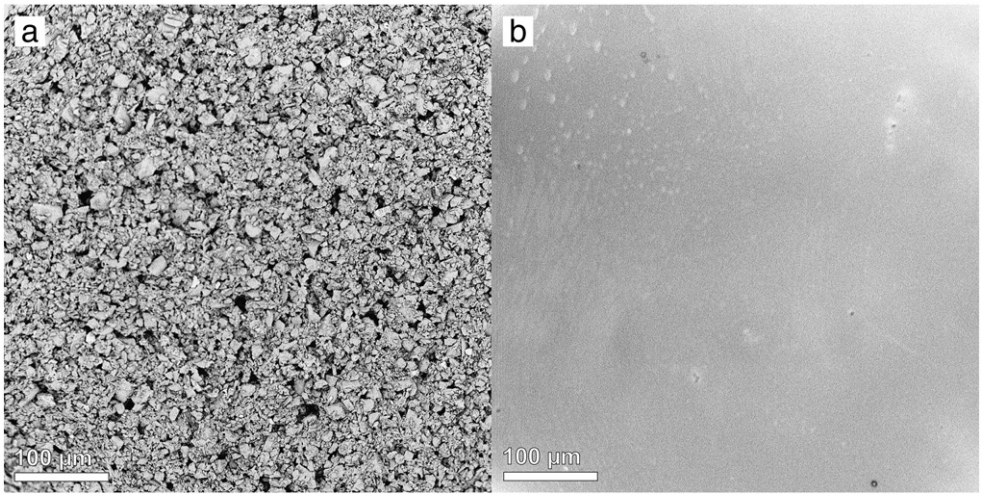

Fig. 3. SEM images of a) uncoated electrode surface and b) coated electrode surface.

the transient responses of the coated electrodes are different for the forward and reverse scans, with a slower change in capacitance at the beginning of the reverse scan. This is thought to be a result of the expulsion of anions from the pores through the cation exchange polymer matrix, which would cause additional resistance to the adsorption process.

As shown in Fig. 6a and b, the response of electrodes coated with RCP 1 to a change in scan direction is seen to be faster when compared with electrodes coated with polymers RCP 2 and RCP 3. This may be attributed to the high ion-exchange capacity and water uptake of RCP 1 compared with the other copolymers. Surprisingly, this response is also faster than that of the uncoated sample. This may be due to a high PVDF content in the substrate carbon electrode, where the PVDF behaves like a partial, hydrophobic membrane layer that blocks pores, creating additional hindrance to the adsorption/desorption process. Although the polymer coating increases resistance, copolymer penetration into the voids of the carbon substrate may simultaneously reduce the charging resistance by providing better access to the pores due to its hydrophilic properties. The solubility of the PVDF binder in NMP, which is used as a solvent for the polymer coatings, may have also resulted in a partial dissolution and re-drying of the PVDF binder during the polymer coating process, effectively re-casting some of the carbon substrate with both PVDF and random copolymer as a binder.

3.4. Electrochemical analysis — Electrochemical impedance spectroscopy

Electrochemical impedance spectroscopy was used to further examine the performance of the electrodes and to measure the charging resistance. The resistance and conductivity of the coating layers were calculated based on the real impedance at the high-frequency intercept of the Nyquist plot. The resistances of the coatings can be seen in Table 2. They have not been normalised to account for the variable thickness of the coatings and as such they do not decrease with increasing IEC. Importantly, the resistances of the RCP 1 and RCP 2 coatings are comparable to Neosepta CMX, which has a resistance of 3.0 $\Omega.cm^2$ [35]. The conductivity of the coatings shown in Table 2 has been calculated based on thickness, and thus is seen to increase with increasing IEC. These values differ to those reported in Table 1 due to the methods of testing; the polymer coating conductivity was measured normal to its exposed surface (through-plane conductivity), while previous measurements with a four-point probe [45] were parallel to the surface (in-plane conductivity), which is known to yield different values.

Electrode charging resistance versus frequency is shown in Fig. 7. This is the resistance to ion transport through the polymer matrix and into the carbon pores, and is calculated as the real impedance minus the ohmic resistance at each frequency. For the uncoated sample, the

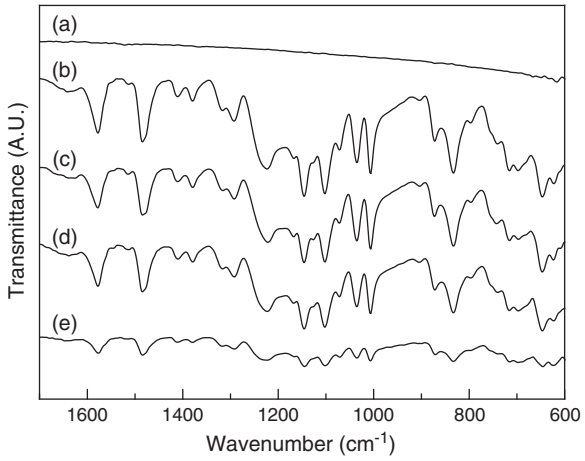

Fig. 4. ATR-FTIR spectra of (a) uncoated carbon electrode, (b) stand-alone membrane, (c) RCP 1 coated electrode, (d) RCP 2 coated electrode and (e) RCP 3 coated electrode.

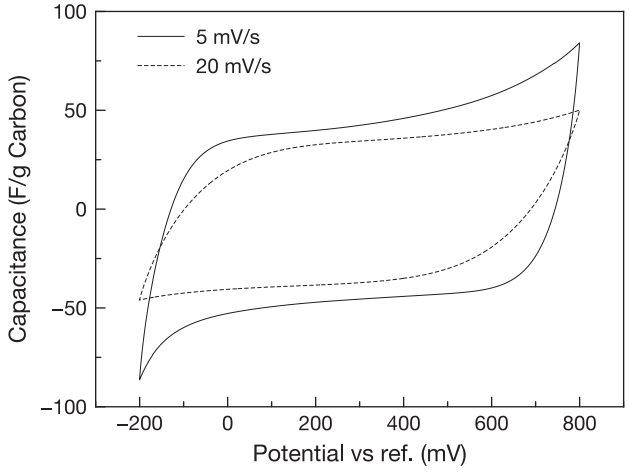

Fig. 5. Specific capacitance of uncoated electrodes measured in 0.5 M NaCl at scan rates of 5 mV/s (solid line) and 20 mV/s (dotted line).

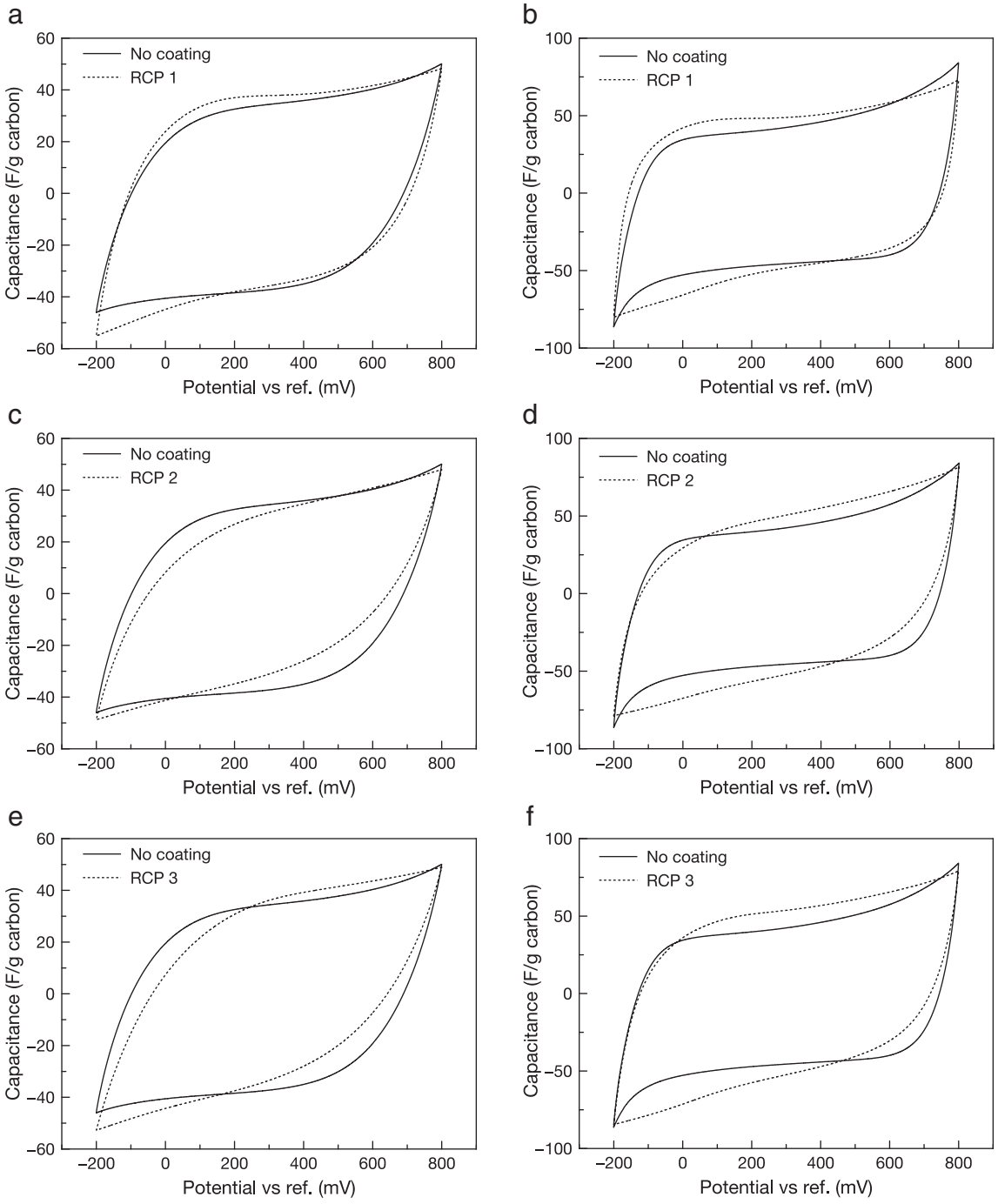

Fig. 6. Specific capacitance of coated electrodes measured in 0.5 M NaCl: a) RCP 1 coating, scan rate = 20 mV/s; b) RCP 1 coating, scan rate = 5 mV/s; c) RCP 2 coating, scan rate = 20 mV/s; d) RCP 2 coating, scan rate = 5 mV/s; e) RCP 3 coating, scan rate = 20 mV/s; f) RCP 3 coating, scan rate = 5 mV/s.

rise in charging resistance at higher frequency compared to the coated samples is likely due to the high PVDF content, which as described above blocks pores and creates additional hindrance to ion adsorption.

Table 2
Electrochemical properties of the coating layers and capacitance of coated and uncoated electrodes, measured using EIS.

Coating	IEC (mmol/g)	Thickness (μm)	Resistance (Ω.cm^2)	Conductivity (mS/cm)	Capacitance (F/g carbon)
RCP 1	2.05	82	3.31	2.48	37.74
RCP 2	1.73	46	2.37	1.94	30.07
RCP 3	1.44	59	9.86	0.60	25.00
No coating	–	–	–	–	32.56

For the coated samples, the onset of charging resistance occurs at higher frequencies for polymer coatings with greater resistance. Although the RCP 1 coated sample has a higher measured resistance and greater thickness than the RCP 2 coated sample, the charging resistance is similar. This result suggests that the higher conductivity and greater water uptake of RCP 1 reduces hindrance to ion transport.

As the frequency approaches 10 mHz, the charging resistance climbs sharply for all coated samples. Here, the impedance response is dominated by the resistance of the coating rather than the capacitive behaviour of the carbon substrate. In light of this, while coating area resistances are comparable to those of commercial membranes, polymer layer thickness must still be optimised to minimise charging resistance while still adequately enhancing electrosorption capacitance.

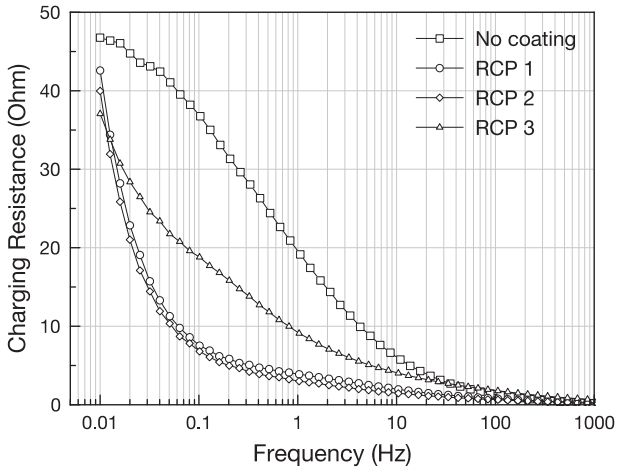

Fig. 7. Charging resistance versus frequency for uncoated and coated electrodes.

Assuming ideal capacitor behaviour, the capacitance of the electrode, C (F) can be derived from the imaginary part of the impedance spectra based on the formula [49]:

$$C = \left| \frac{1}{\omega Z''} \right|$$

Where ω is the frequency and Z″ is the imaginary impedance. The calculated capacitance versus frequency is plotted in Fig. 8, and the capacitance calculated at 10 mHz can be seen in Table 2. The capacitance of the coated samples is seen to increase with IEC, while the influence of the coating layer resistance seems to be less significant. The increased capacitance as a function of IEC is likely a result of greater water uptake, which reduces resistance to ion transport through the swollen hydrophilic channels of the polymer, encouraging greater pore access. Furthermore, the higher water uptake promotes a region of concentrated electrolyte storage in the polymer layer. As the charge buildup that results from electrical double layer formation is known to increase with concentration, increased electrolyte concentration directly adjacent to the carbon electrode in the polymer can increase its capacitance.

4. Conclusions

Activated carbon electrodes coated with cation exchange random copolymers were successfully fabricated, with the coating layer strongly adhering to the carbon. Cyclic voltammetry results have shown that in the case of the most conductive coating, charge is seen to build up at a faster rate than uncoated samples, despite the additional resistance of the coating. EIS results indicate that the charging resistance and capacitance of the coated electrodes are influenced by both conductivity and water uptake. Since the conductivity and water uptake are strong functions of IEC, suitable polymer design to maximise IEC while retaining mechanical stability is a crucial parameter in enhancing the performance of activated carbon electrodes. In light of this, RCP 1 is seen to appreciably enhance the electrosorption performance of the activated carbon electrodes.

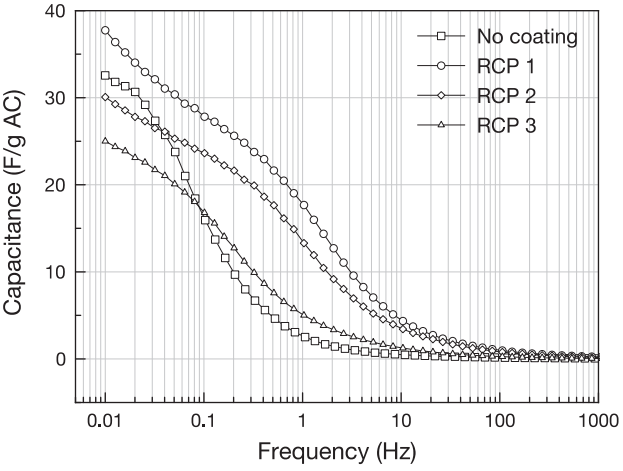

Fig. 8. Capacitance versus frequency for uncoated and coated electrodes.

The polymer coatings are seen to influence the resistance of the carbon electrodes, causing a sharp rise in charging resistance at low frequencies during EIS testing. The optimisation of coating thickness therefore becomes important in reducing the additional resistance created by the coating layer. Further work will require a detailed EIS investigation into these systems, in particular systematically varying the polymer coating thickness, so that an EIS model can be developed and fitted to the data with a high degree of confidence. This will enable the elucidation of the relative contributions of the resistance and capacitive elements of the EIS spectra.

A high PVDF binder content can also reduce capacitance and increase charging resistance, slowing the build up of ions at the electrode–solution interface. However, the coating of electrodes with an ion exchange polymer may offset this phenomenon, possibly through copolymer penetration into the carbon substrate in addition to acting as a charge barrier layer.

These results indicate that the random copolymer coatings, although increasing overall resistance, can be used to improve the ion transport into the pores of the electrodes.

Acknowledgements

The authors acknowledge the financial support of the National Centre of Excellence in Desalination Australia, which is funded by the Australian Government through the Water for the Future Initiative.

References

[1] J.C. Farmer, Method and Apparatus for Capacitive Deionization, Electrochemical Purification, and Regeneration of Electrodes, 1995.
[2] M.A. Anderson, A.L. Cudero, J. Palma, Capacitive deionization as an electrochemical means of saving energy and delivering clean water. Comparison to present desalination practices: will it compete? Electrochim. Acta 55 (2010) 3845–3856.
[3] Australian Desalination Research Roadmap, National Centre of Excellence in Desalination Australia, 2012.
[4] K.-K. Park, J.-B. Lee, P.-Y. Park, S.-W. Yoon, J.-S. Moon, H.-M. Eum, C.-W. Lee, Development of a carbon sheet electrode for electrosorption desalination, Desalination 206 (2007) 86–91.
[5] L. Zou, G. Morris, D. Qi, Using activated carbon electrode in electrosorptive deionisation of brackish water, Desalination 225 (2008) 329–340.
[6] J. Lee, K. Park, S. Yoon, P. Park, K. Park, C. Lee, Desalination performance of a carbon-based composite electrode, Desalination 237 (2009) 155–161.
[7] J.H. Choi, Fabrication of a carbon electrode using activated carbon powder and application to the capacitive deionization process, Sep. Purif. Technol. 70 (2010) 362–366.
[8] C.-H. Hou, J.-F. Huang, H.-R. Lin, B.-Y. Wang, Preparation of activated carbon sheet electrode assisted electrosorption process, J. Taiwan Inst. Chem. Eng. 43 (2012) 473–479.
[9] G. Wang, C. Pan, L. Wang, Q. Dong, C. Yu, Z. Zhao, J. Qiu, Activated carbon nanofiber webs made by electrospinning for capacitive deionization, Electrochim. Acta 69 (2012) 65–70.
[10] B.-H. Park, Y.-J. Kim, J.-S. Park, J. Choi, Capacitive deionization using a carbon electrode prepared with water-soluble poly(vinyl alcohol) binder, J. Ind. Eng. Chem. 17 (2011) 717–722.
[11] I. Villar, S. Roldan, V. Ruiz, M. Granda, C. Blanco, R. Menéndez, R. Santamaría, Capacitive deionization of NaCl solutions with modified activated carbon electrodes†, Energy Fuels 24 (2010) 3329–3333.
[12] S. Nadakatti, M. Tendulkar, M. Kadam, Use of mesoporous conductive carbon black to enhance performance of activated carbon electrodes in capacitive deionization technology, Desalination 268 (2011) 182–188.
[13] X.Z. Wang, M.G. Li, Y.W. Chen, R.M. Cheng, S.M. Huang, L.K. Pan, Z. Sun, Electrosorption of ions from aqueous solutions with carbon nanotubes and nanofibers composite film electrodes, Appl. Phys. Lett. 89 (2006) 053127.
[14] L. Zou, Developing nano-structured carbon electrodes for capacitive brackish water desalination, in: R.Y. Ning (Ed.), Expanding Issues in Desalination, InTech, 2011.

[15] M.-W. Ryoo, J.-H. Kim, G. Seo, Role of titania incorporated on activated carbon cloth for capacitive deionization of NaCl solution, J. Colloid Interface Sci. 264 (2003) 414–419.
[16] M.-W. Ryoo, G. Seo, Improvement in capacitive deionization function of activated carbon cloth by titania modification, Water Res. 37 (2003) 1527–1534.
[17] H.-J. Ahn, J.-H. Lee, Y. Jeong, J.-H. Lee, C.-S. Chi, H.-J. Oh, Nanostructured carbon cloth electrode for desalination from aqueous solutions, Mater. Sci. Eng. A 449–451 (2007) 841–845.
[18] H. Oh, J. Lee, H. Ahn, Y. Jeong, Y. Kim, C. Chi, Nanoporous activated carbon cloth for capacitive deionization of aqueous solution, Thin Solid Films 515 (2006) 220–225.
[19] M.T.Z. Myint, J. Dutta, Fabrication of zinc oxide nanorods modified activated carbon cloth electrode for desalination of brackish water using capacitive deionization approach, Desalination 305 (2012) 24–30.
[20] M.Z. Bazant, K. Thornton, A. Ajdari, Diffuse-charge dynamics in electrochemical systems, Phys. Rev. E. 70 (2004) 021506.
[21] P.M. Biesheuvel, Thermodynamic cycle analysis for capacitive deionization, J. Colloid Interface Sci. 332 (2009) 258–264.
[22] A.M. Johnson, J. Newman, Desalting by means of porous carbon electrodes, J. Electrochem. Soc. 118 (1971) 510–517.
[23] Y. Oren, A. Soffer, Water desalting by means of electrochemical parametric pumping. I. The equilibrium properties of a batch unit cell, J. Appl. Electrochem. 13 (1983) 473–487.
[24] M.D. Andelman, G.S. Walker, Charge Barrier Flow-through Capacitor, in, United States, 2004.
[25] J. Lee, K. Park, H. Eum, C. Lee, Desalination of a thermal power plant wastewater by membrane capacitive deionization, Desalination 196 (2006) 125–134.
[26] N.-S. Kwak, J.S. Koo, T.S. Hwang, E.M. Choi, Synthesis and electrical properties of NaSS-MAA-MMA cation exchange membranes for membrane capacitive deionization (MCDI), Desalination 285 (2012) 138–146.
[27] M. Andelman, Flow through capacitor basics, Sep. Purif. Technol. 80 (2011) 262–269.
[28] H. Li, L. Zou, Ion-exchange membrane capacitive deionization: a new strategy for brackish water desalination, Desalination 275 (2011) 62–66.
[29] R. Zhao, P.M. Biesheuvel, A. van der Wal, Energy consumption and constant current operation in membrane capacitive deionization, Energy Environ. Sci. 5 (2012) 9520.
[30] R. Zhao, O. Satpradit, H.H. Rijnaarts, P.M. Biesheuvel, A. van der Wal, Optimization of salt adsorption rate in membrane capacitive deionization, Water Res. 47 (2013) 1941–1952.
[31] P.M. Biesheuvel, A. van der Wal, Membrane capacitive deionization, J. Membr. Sci. 346 (2010) 256–262.
[32] Y.J. Kim, J.H. Choi, Enhanced desalination efficiency in capacitive deionization with an ion-selective membrane, Sep. Purif. Technol. 71 (2010) 70–75.
[33] Y.J. Kim, J. Hur, W. Bae, J.H. Choi, Desalination of brackish water containing oil compound by capacitive deionization process, Desalination 253 (2010) 119–123.
[34] J.Y. Lee, S.J. Seo, S.H. Yun, S.H. Moon, Preparation of ion exchanger layered electrodes for advanced membrane capacitive deionization (MCDI), Water Res. 45 (2011) 5375–5380.
[35] ASTOM Corporation, Neosepta, http://www.astom-corp.jp/en/en-main2-neosepta.html 2004.
[36] J.S. Kim, J.H. Choi, Fabrication and characterization of a carbon electrode coated with cation-exchange polymer for the membrane capacitive deionization applications, J. Membr. Sci. 355 (2010) 85–90.
[37] H.B. Park, B.D. Freeman, Z.B. Zhang, M. Sankir, J.E. McGrath, Highly chlorine-tolerant polymers for desalination, Angew. Chem. Int. Ed. Engl. 47 (2008) 6019–6024.
[38] M. Paul, H.B. Park, B.D. Freeman, A. Roy, J.E. McGrath, J.S. Riffle, Synthesis and crosslinking of partially disulfonated poly(arylene ether sulfone) random copolymers as candidates for chlorine resistant reverse osmosis membranes, Polymer 49 (2008) 2243–2252.
[39] W. Xie, H.B. Park, J. Cook, C.H. Lee, G. Byun, B.D. Freeman, J.E. McGrath, Advances in membrane materials: desalination membranes based on directly copolymerized disulfonated poly(arylene ether sulfone) random copolymers, Water Sci. Technol. 61 (2010) 619–624.
[40] W. Xie, J. Cook, H.B. Park, B.D. Freeman, C.H. Lee, J.E. McGrath, Fundamental salt and water transport properties in directly copolymerized disulfonated poly(arylene ether sulfone) random copolymers, Polymer 52 (2011) 2032–2043.
[41] W. Xie, G.M. Geise, B.D. Freeman, C.H. Lee, J.E. McGrath, Influence of processing history on water and salt transport properties of disulfonated polysulfone random copolymers, Polymer 53 (2012) 1581–1592.
[42] W.L. Harrison, Synthesis and Characterization of Sulfonated poly(arylene ether sulfone) Copolymers via Direct Copolymerization: Candidates for Proton Exchange Membrane Fuel Cells, in, Virginia Polytechnic Institute and State University, 2002.
[43] C. Vogel, H. Komber, A. Quetschke, W. Butwilowski, A. Pötschke, K. Schlenstedt, J. Meier-Haack, Side-chain sulfonated random and multiblock poly(ether sulfone)s for PEM applications, React. Funct. Polym. 71 (2011) 828–842.
[44] C. Vogel, J. Meier-Haack, Preparation of ion-exchange materials and membranes, Desalination 342 (2014) 156–174.
[45] B.M. Asquith, J. Meier-Haack, C. Vogel, W. Butwilowski, B.P. Ladewig, Side-chain sulfonated copolymer cation exchange membranes for electro-driven desalination applications, Desalination 324 (2013) 93–98.
[46] S. Brunauer, The adsorption of gases and vapors, Physical Adsorption, Vol. I, Princeton University Press, Princeton, NJ, 1943.
[47] J. Rouquerol, P. Llewellyn, F. Rouquerol, Is the BET equation applicable to microporous adsorbents? in: P Llewellyn, F. Rodriguez-Reinoso, J. Rouquerol, N. Seaton (Eds.), Stud. Surf. Sci. Catal.Elsevier, 2007, pp. 49–56.
[48] A.J. Bard, L.R. Faulkner, Electrochemical Methods: Fundamentals and Applications, John Wiley, New York, 2001.
[49] P.M.S. Monk, Fundamentals of Electroanalytical Chemistry, Wiley, Chichester, 2001.